EUROPEAN ORGANIZATION FOR NUCLEAR RESEARCH

CERN-EP/84-106
24 August 1984

PHOTOPRODUCTION OF ϕ MESONS BY LINEARLY POLARIZED PHOTONS OF ENERGY 20-40 GeV AND FURTHER EVIDENCE FOR A PHOTOPRODUCED HIGH-MASS KK ENHANCEMENT

The Omega Photon Collaboration

M. Atkinson[7], T.J. Axon[5], D. Barberis[5], T.J. Brodbeck[4], G.R. Brookes[8], J.J. Bunn[8], P.J. Bussey[3], A.B. Clegg[4], J.B. Dainton[3], M. Davenport[7], B. Dickinson[5], B. Diekmann[1], A. Donnachie[5], R.J. Ellison[5], P. Flower[7], P.J. Flynn[4], W. Galbraith[8], K. Heinloth[1], R.C.W. Henderson[4], R.E. Hughes-Jones[5], J.S. Hutton[7], M. Ibbotson[5], H.-P. Jakob[1], M. Jung[1], B.R. Kumar[7], J. Laberrigue[6], G.D. Lafferty[5], J.B. Lane[5], J.-C. Lassalle[2], J.M. Lévy[6], V. Liebenau[1], R. McClatchey[8], D. Mercer[5], J.A.G. Morris[7], J.V. Morris[7], D. Newton[4], C. Paterson[3], G.N. Patrick[2], E. Paul[1], C. Raine[3], M. Reidenbach[1], H. Rotscheidt[1], A. Schlösser[1], P.H. Sharp[7], I.O. Skillicorn[3], K.M. Smith[3], K.M. Storr[2], R.J. Thompson[5], Ch. de la Vaissière[6], A.P. Waite[5], M.F. Worsell[5] and T.P. Yiou[6]

Bonn[1]-CERN[2]-Glasgow[3]-Lancaster[4]-Manchester[5]-Paris VI[6]-Rutherford[7]-Sheffield[8]

ABSTRACT

A study of ϕ-meson photoproduction by partially polarized photons of energy 20-40 GeV is reported. The production mechanism is found to conserve s-channel helicity and to proceed via natural-parity exchange in the t channel. In the photoproduction of high-mass K^+K^- states with photons of energy 20-70 GeV, there is evidence for an enhancement at a mass of 1.76 GeV with width 0.08 GeV.

(To be submitted to Z. Phys. C)

0014P/GDL/sm

1. INTRODUCTION

The photoproduction of ϕ mesons at photon energies of 20-40 GeV has been studied previously [1]. In this paper measurements of ϕ photoproduction with partially polarized photons are presented; this enables separation of the contributions to the total cross-section from natural and unnatural parity exchange.

The high-mass KK spectrum is of considerable interest in the search for possible radial excitations of the ϕ meson. Further evidence is reported here for an enhancement at 1.76 GeV, already observed in a previous photoproduction experiment [2].

2. EXPERIMENT AND DATA REDUCTION

The data presented here originate from an experiment (WA57) using the CERN SPS tagged photon beam at the Omega spectrometer. A silicon crystal was used as a target to produce, by means of coherent bremsstrahlung, linearly polarized photons of energy 20 to 70 GeV with a resulting mean polarization of 30% [3]. A full description of the apparatus can be found in [4].

The data for the reaction

$$\gamma p \rightarrow K^+K^-p \qquad (1)$$

originate from a trigger requiring two or three forward charged particles. Electron-positron pairs were rejected by demanding no signal from a shower counter array in the median plane downstream of the spectrometer. Offline selection required two or three charged particles to be reconstructed to a single main vertex within the hydrogen target with charge balance 0 or +1 (in the latter case one positive track had to be consistent with the hypothesis of a recoil proton). A large-aperture 32-cell gas threshold Cerenkov counter downstream of the Omega spectrometer was used for charged particle identification. The thresholds for π,K and p were 5.6, 17 and 32 GeV/c, respectively. The offline identification of charged kaons was made by requiring a track with momentum between 5.6 and 17 GeV/c with a correlated signal between slats from two hodoscopes in front of and behind the Cerenkov counter together with no light from the corresponding Cerenkov

cell. For ϕ photoproduction both fast tracks had to fulfill these criteria (in the following called "KK2" events). To increase statistics in the high KK mass region (above 1.046 GeV) events were also accepted where only one track was identified as a charged kaon whilst the other was required to have momentum > 20 GeV/c and to produce light in the Cerenkov counter. This latter data sample is called "KK1" and covers the photon energy range up to 70 GeV.

Final selection of reaction (1) required the energy difference $|\Delta E| = |E_\gamma - E_{KK} - T_p|$ to be less than 1.5 GeV (T_p is the kinetic energy of the recoil proton and is only included when measured). The quantity ΔE is shown in Fig. 1a for K^+K^- masses in the ϕ range (1.002 to 1.046 GeV) and in Fig. 1b for K^+K^- masses above 1.046 GeV. A subsample of events have one or more signals in the photon detector downstream of the Cerenkov counter which cannot be reconstructed to form π^o or η mesons. Figure 1c (ϕ range) and Fig. 1d (high masses) show ΔE for these events. The inelastic contamination within $|\Delta E| < 1.5$ GeV is not changed significantly for the ϕ mass range but is considerably increased for the high-mass events. Consequently, the events contributing to Fig. 1d were rejected.

3. ACCEPTANCE

The geometrical acceptance of the apparatus was obtained by a Monte Carlo simulation assuming diffractive production of the K^+K^- system [energy independent total cross-section and differential cross-section $d\sigma/dt \propto \exp(-b|t|)$, with $b = 5\ \text{GeV}^{-2}$]. For the ϕ meson a decay angular distribution in the helicity frame of the form $W(\cos\theta) \propto \sin^2\theta$ was used as input (see Ref. 5 for the definition of the angles). For the high KK mass region the decay angular distribution was assumed to be isotropic. The acceptance program accounted for losses due to the trigger requirements, pattern recognition and vertex reconstruction as well as for hadron rejection by the electromagnetic shower counter and inefficiencies of the kaon reconstruction.

4. EXPERIMENTAL RESULTS

4.1 ϕ-meson production

Figure 2 shows the K^+K^- mass spectrum for the KK2 events indicating a strong $\phi(1019)$ signal. The dashed line represents the geometrical acceptance.

The total of 1135 ϕ-meson events ($1.002 < m_{KK} < 1.046$ GeV) deduced from this spectrum corresponds to a production cross-section of

$$\sigma(\gamma p \to \phi p) \cdot B(\phi \to K^+K^-) = 224 \pm 7 \pm 50 \text{ nb}$$

(where the quoted errors are statistical and systematic, respectively).

The four-momentum transfer, $|t|$, distribution is well fitted by an exponential form [$d\sigma/dt = d\sigma/dt|_{t=o} \times \exp(-b|t|)$] giving the following values for $d\sigma/dt|_{t=o}$ and b respectively [taking $B(\phi \to K^+K^-) = 48\%$] in two ranges of incident photon energy:

E_γ = 20–27 GeV $\quad d\sigma/dt|_{t=o} = 2.01 \pm 0.19$ μb

$\quad b = 5.26 \pm 0.30$ GeV^{-2}

E_γ = 27–40 GeV $\quad d\sigma/dt|_{t=o} = 2.39 \pm 0.22$ μb

$\quad b = 5.02 \pm 0.26$ GeV^{-2}

(the quoted errors are statistical errors given by the fits). All values found are compatible with earlier measurements [1].

Figures 3a and 3b show the decay angular distribution of the ϕ meson measured in the s-channel helicity frame in terms of cos θ and $\psi = \Phi - \phi$, the K^+ direction taken as the analyser (see Ref. 5). For the diffractive photoproduction of an s-channel helicity conserving $J^P = 1^-$ state with polarized photons this decay angular distribution is expected to be [6]:

$$W(\cos\theta, \psi) \propto \sin^2\theta \, (1 + P_\gamma \cos^2\psi) \, .$$

The curves in Figs. 3a and 3b show the result of a fit of the data to $W(\cos\theta, \psi)$. The curves describe the data well and the fit gives a mean photon polarization of $P_\gamma = 0.29 \pm 0.07$ in agreement with the value of 30% calculated from the photon tagging system [3]. To obtain the nine spin-density matrix elements describing the ϕ production, the acceptance-corrected spherical harmonic moments of the decay angular distribution were evaluated. The results are listed in Table 1 and are consistent with the

expectation for s-channel helicity conservation: there are only two non-vanishing matrix elements, $\rho^1_{1-1} = -\mathrm{Im}\ \rho^2_{1-1} = 1/2$. The contributions to the total cross-section from natural (σ^N) and unnatural (σ^U) parity exchange in the t-channel have been calculated from

$$P_\sigma = \frac{\sigma^N - \sigma^U}{\sigma_{tot}} = 2\rho^1_{1-1} - \rho^1_{oo}$$

where

$$\sigma_{tot} = \sigma^N + \sigma^U$$

giving

$$P_\sigma = 0.94 \pm 0.34 \ .$$

This is consistent with the dominance of natural-parity exchange in the production process.

4.2 Production of high-mass K^+K^- states

High-mass K^+K^- pairs are of special interest because of the possible existence of radial excitations of the ϕ meson. An earlier experiment at the CERN Omega Spectrometer has shown evidence for an enhancement at 1.748 ± 0.011 GeV with a width of 80 ± 30 MeV in the invariant K^+K^- mass spectrum [2]. Further evidence for this enhancement is now found in the present experiment where a structure is observed at the same K^+K^- mass with a comparable width.

In order to provide a clean KK event sample in the high KK mass region, the following background processes, which may simulate high-mass K^+K^- events, were considered:

$$\gamma p \to e^+e^-p \qquad (2)$$

$$\gamma p \to p\bar{p}p \qquad (3)$$

$$\gamma p \to \pi^+\pi^-p \ . \qquad (4)$$

Events from reaction (2) are expected to peak at the KK threshold and are efficiently rejected by the trigger and offline selection criteria; no threshold peaking is seen in any of the mass spectra.

Events from reaction (3) only contribute to the KK2 event sample. This background is evaluated using our fully reconstructed three-prong events, applying the same kinematic cuts as described in Ref. 1, and is found to be at most 20% varying smoothly over the whole mass range.

Contamination by reaction (4) is found to be important for the KK1 event sample because of inefficiency of the Cerenkov counter. This can be seen in Figs. 4a and 4b which show the acceptance-corrected KK mass spectra for KK2 and KK1 events, respectively. This background originates mainly from the decay of the ρ^o meson which gives a peak in the KK mass spectrum at 1.25 GeV (see Fig. 4b), falling rapidly with increasing KK mass. Figure 5 shows the result of subtracting the normalized distribution of Fig. 4a from that of 4b and indicates that the ρ^o reflection is unimportant at K^+K^- masses above 1.4 GeV. Also, the fact that the data of Fig. 5 are consistent with zero outside the ρ^o reflection shows that the acceptance corrections for KK1 and KK2 events are well understood. This is also apparent from the fact that the cross-section and shape of the ρ^o reflection in these KK1 data are in agreement with expectations from previous measurements of reaction (4) in the same energy range [7].

Figures 6a and 6b give the K^+K^- mass distributions for KK2 and KK1 events, respectively. Both distributions are corrected for the corresponding acceptance (shown as the dotted lines). Figure 7 shows the sum of these two mass distributions indicating a structure at 1.75 GeV. The full line corresponds to a fit to this mass distribution with a simple Breit-Wigner for the enhancement and a third-order polynomial for the background. The parameters for the Breit-Wigner from the fit are:

$$m = 1.76 \pm 0.02 \text{ GeV}$$

$$\Gamma = 0.08 \pm 0.04 \text{ GeV} .$$

The statistical significance of the peak over the background is $\sim 3.5\sigma$ and the fit has $\chi^2 = 12$ for 20 degrees of freedom.

To investigate the spin-parity of this structure, a fit was made to the acceptance-corrected cos θ decay angular distributions for three ranges of KK mass according to:

$$W(\cos\theta) = A[(1-B)\cos^2\theta + (1+B)\sin^2\theta]$$

with the result

$$1.4 < m_{KK} < 1.6 \text{ GeV} \qquad B = 0.01 \pm 0.24$$

$$1.6 < m_{KK} < 1.9 \text{ GeV} \qquad B = 0.28 \pm 0.37$$

$$1.9 < m_{KK} < 2.1 \text{ GeV} \qquad B = -0.80 \pm 0.12 \ .$$

These results indicate a mainly flat distribution below and in the mass range of the structure and a $\cos^2\theta$ component at higher masses. For the decay of an s-channel helicity conserving $J^P = 1^-$ state this decay angular distribution would be purely $\sin^2\theta$. However no conclusions can be drawn from the distributions obtained here because any such 1^- state might be hidden by contributions of non-resonant K^+K^- systems with different spin parities or production mechanisms.

Taking the measured slope of the t distribution ($b = 4.6 \pm 0.2$ GeV^{-2} for $1.6 < m_{KK} < 1.9$ GeV) and assuming a flat decay angular distribution for the acceptance calculation, the cross-section for this enhancement is found to be

$$\sigma \cdot B = 10 \pm 2.5 \pm 3.5 \text{ nb}$$

if there is no interference between the Breit-Wigner peak and the background. If, instead, the decay angular distribution is taken to be $\propto \sin^2\theta$ this cross-section decreases by ~ 30%.

The simplest interpretation of this structure is as a radial excitation of the $\phi(1019)$ meson. However no firm conclusions can be drawn from this data as to whether or not the observed signal is the result of interference of a narrow $\phi'(1680)$, as reported in the reaction $e^+e^- \to K^{*o}K^o$ [8], with other vector mesons, but the absence of any narrow resonances in

analyses of the reactions $\gamma p \to K^{*} Kp$ [9] and $\gamma p \to \omega \pi^{+} \pi^{-} p$ [10] in the present experiment points against such an interpretation.

5. CONCLUSIONS

Previous work on the photoproduction of ϕ mesons in the photon energy range 20–40 GeV has been extended in this experiment by the use of linearly polarized photons. In addition to confirming that the production mechanism conserves s-channel helicity, the present work has shown that natural parity dominates, the asymmetry parameter, P_{σ}, being

$$P_{\sigma} = \frac{\sigma^{N} - \sigma^{U}}{\sigma^{N} + \sigma^{U}} = 0.94 \pm 0.34$$

where σ^{N} and σ^{U} are the contributions to the total cross-section from natural and unnatural parity exchange respectively in the t channel.

An enhancement in the $K^{+}K^{-}$ mass spectrum with mass 1.76 ± 0.02 GeV and width 0.08 ± 0.04 GeV has been observed. With the assumption that there is no interference with the background, the production cross-section times branching ratio to $K^{+}K^{-}$ is 10 ± 2.5 ± 3.5 nb. The simplest interpretation of the enhancement is that it is a radial excitation of the $\phi(1019)$.

REFERENCES

[1] D. Aston et al., Nucl. Phys. B172 (1980) 1.

[2] D. Aston et al., Phys. Lett. 104B (1981) 231.

[3] P.J. Bussey et al., Nucl. Instrum. Methods 211 (1983) 301.
D. Aston et al., Nucl. Instrum. Methods 197 (1982) 87.

[4] M. Atkinson et al., Nucl. Phys. B231 (1984) 15.

[5] J. Ballam et al., Phys. Rev. D 7 (1973) 3150.

[6] K. Schilling et al., Nucl. Phys. B15 (1970) 397.

[7] D. Aston et al., Nucl. Phys. B209 (1982) 56.

[8] J. Buon et al., Phys. Lett. 118B (1982) 221.

[9] M. Atkinson et al., Nucl. Phys. B231 (1984) 1.

[10] M. Atkinson et al., Nucl. Phys. B229 (1983) 269.

Table 1

ϕ meson spin-density matrix elements
evaluated in the s-channel helicity frame

ρ^0_{00}	0.0332 ± 0.0357
Re ρ^0_{10}	-0.0169 ± 0.0204
ρ^0_{1-1}	0.0214 ± 0.0319
ρ^1_{11}	0.0207 ± 0.1093
ρ^1_{00}	0.0253 ± 0.0931
Re ρ^1_{10}	-0.1275 ± 0.1050
ρ^1_{1-1}	0.4838 ± 0.1648
Im ρ^2_{10}	0.1410 ± 0.0928
Im ρ^2_{1-1}	-0.5708 ± 0.1806

Figure captions

Fig. 1 : Distribution of energy difference, ΔE, for KK2 events in the ϕ mass region ($1.002 < m_{KK} < 1.046$ GeV) (Fig. 1a) and KK2 + KK1 events above the ϕ mass ($m_{KK} > 1.046$ GeV) (Fig. 1b). Figures 1c and 1d are explained in the text.

Fig. 2 : K^+K^- mass spectrum for KK2 events.

Fig. 3 : a) Distribution of cos θ for ϕ-meson decay in the helicity frame.
b) Distribution of ψ for ϕ-meson decay.
The curves are described in the text.

Fig. 3 : a) K^+K^- mass spectrum, corrected for acceptance, for KK2 events above the ϕ mass region.
b) The same as Fig. 4a for KK1 events.

Fig. 5 : Distribution of subtracted mass spectra of Figs. 4b and 4a.

Fig. 6 : a) Invariant mass of K^+K^- for KK2 events corrected for acceptance. The dashed line shows the correction used.
b) Same as for Fig. 6a for KK1 events.

Fig. 7 : Sum of acceptance-corrected K^+K^- mass distributions for KK2 and KK1 events. The full line corresponds to a fit to this distribution as described in the text.

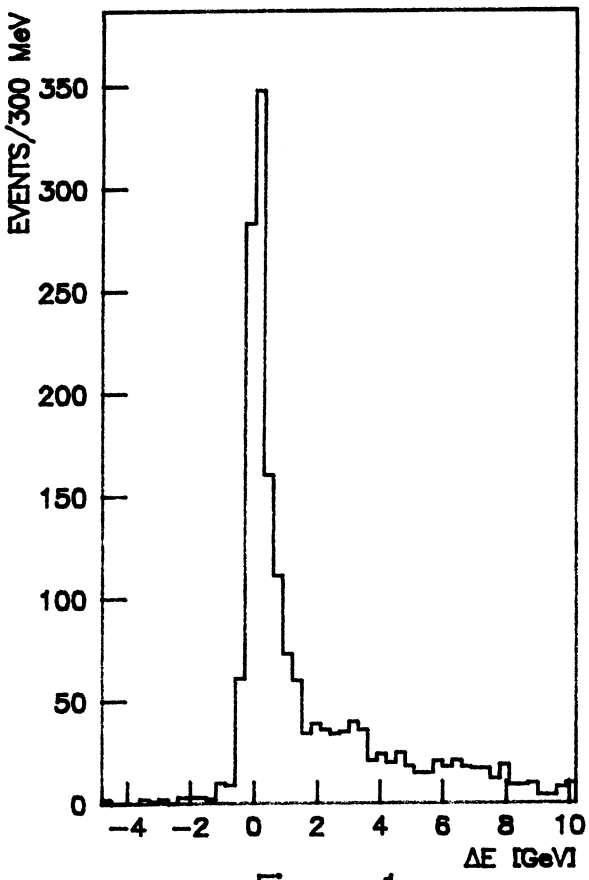

Figure 1a

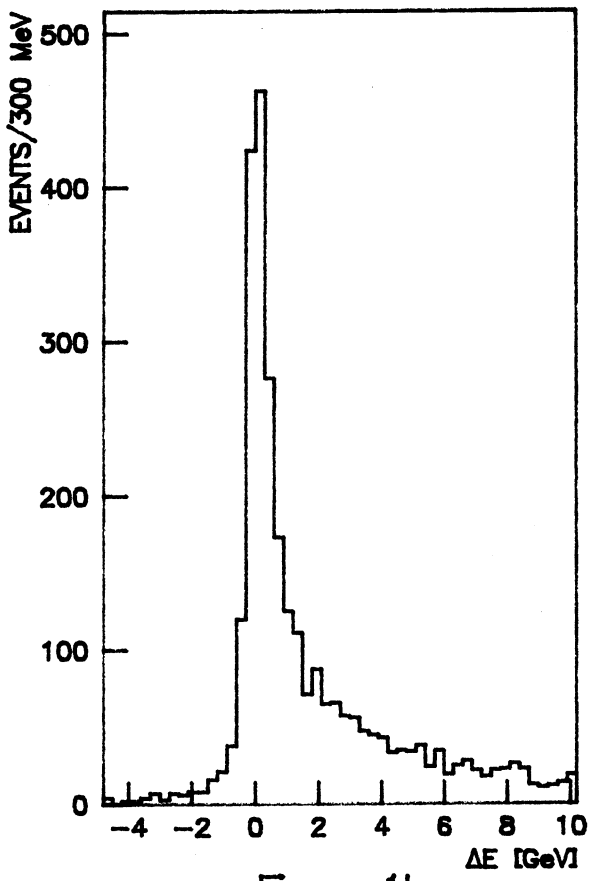

Figure 1b

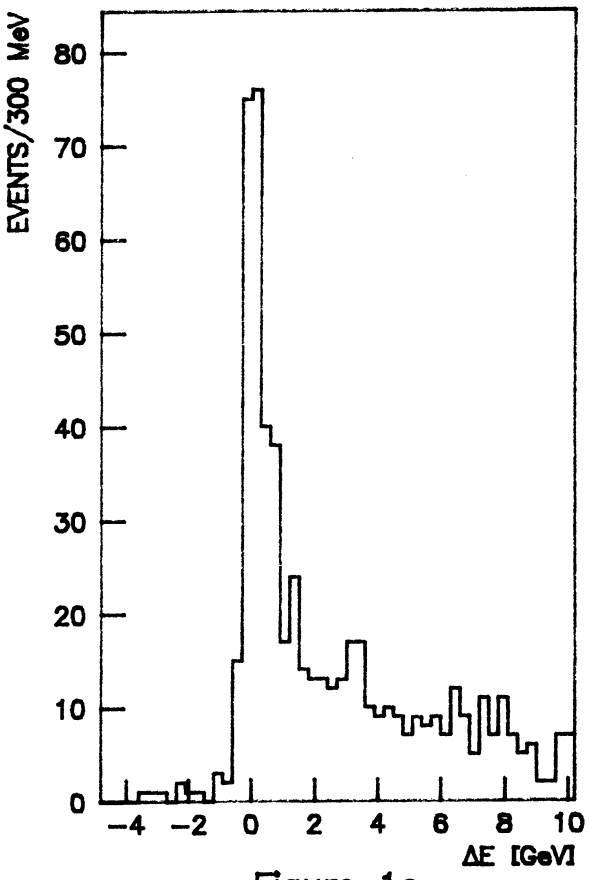

Figure 1c

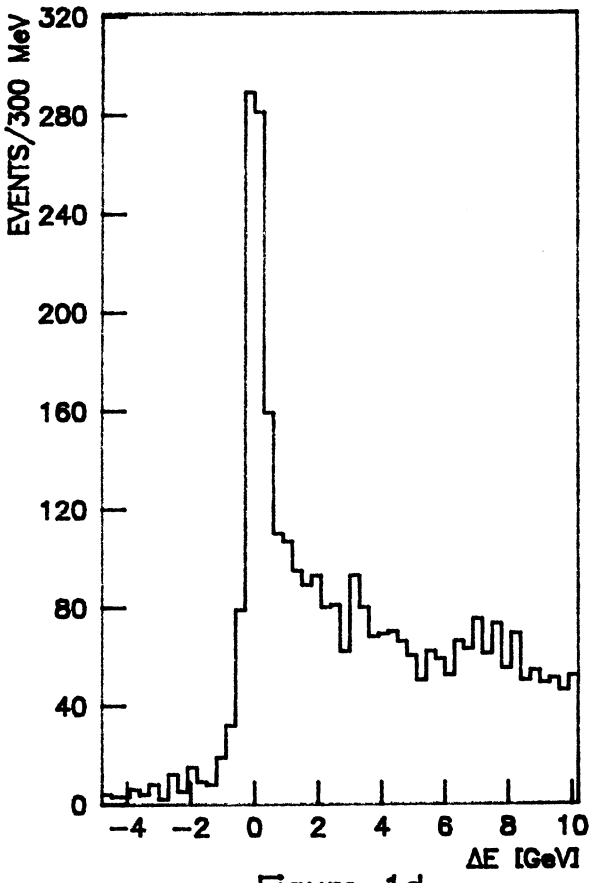

Figure 1d

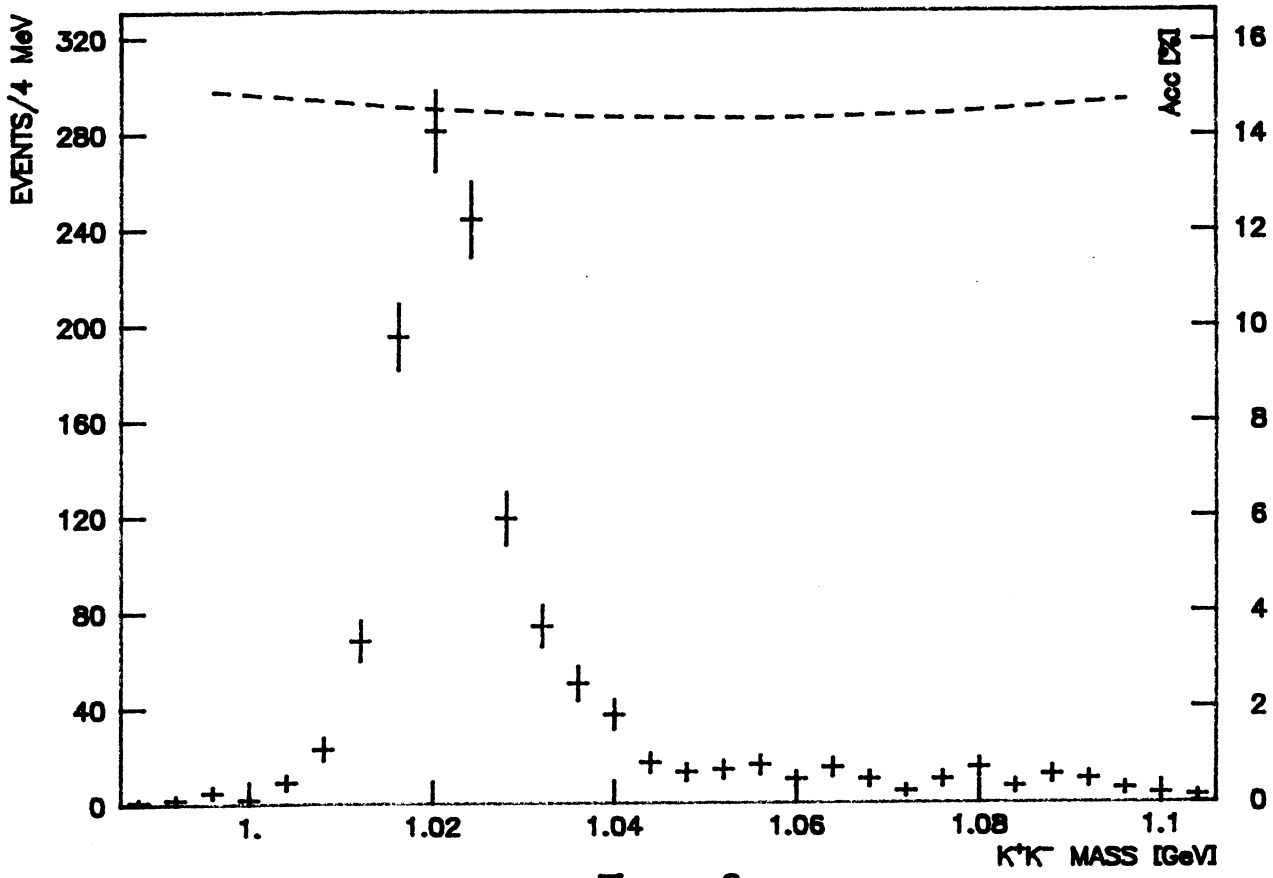

Figure 2

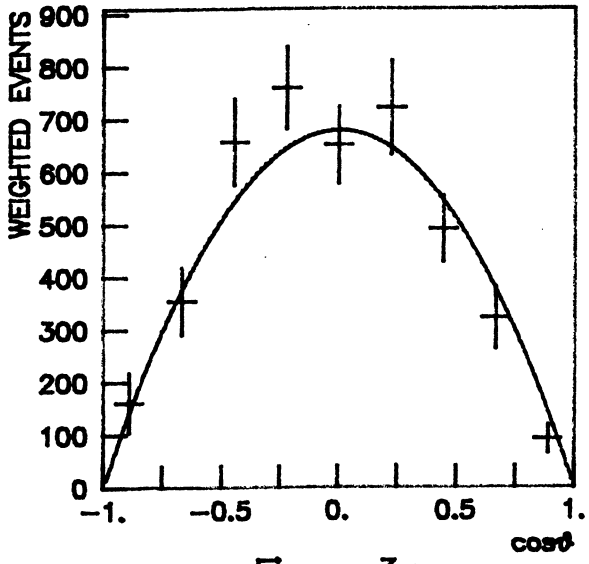

Figure 3a

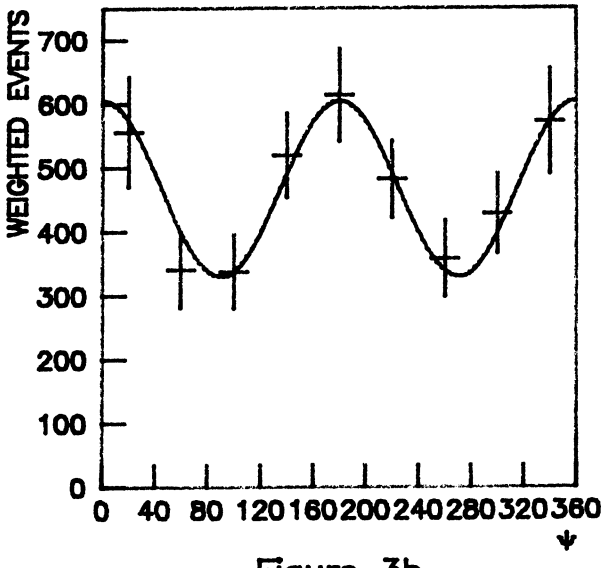

Figure 3b

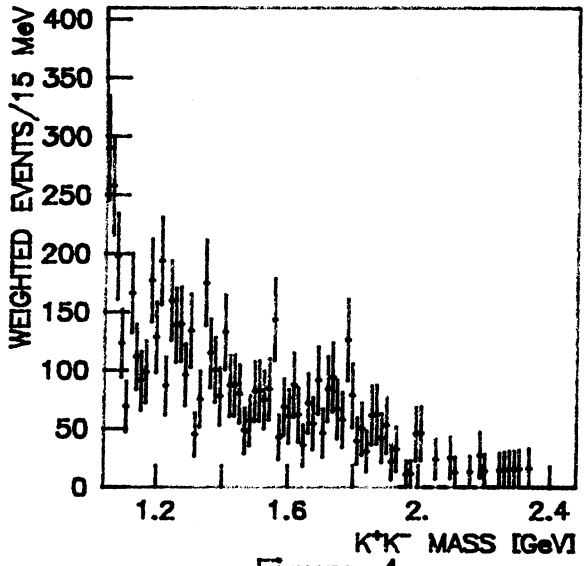

Figure 4a

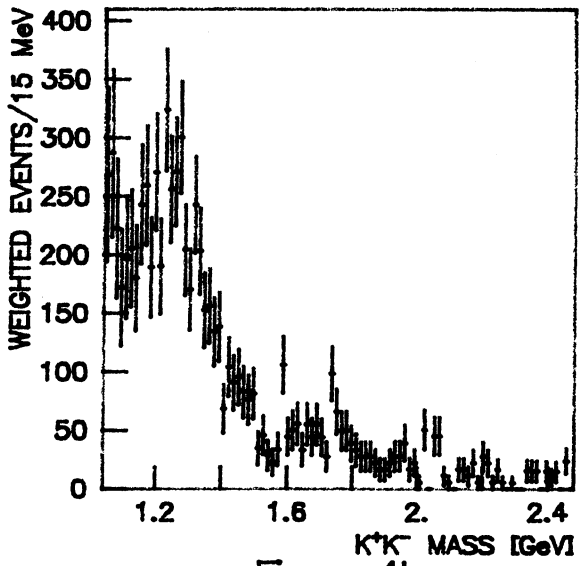

Figure 4b

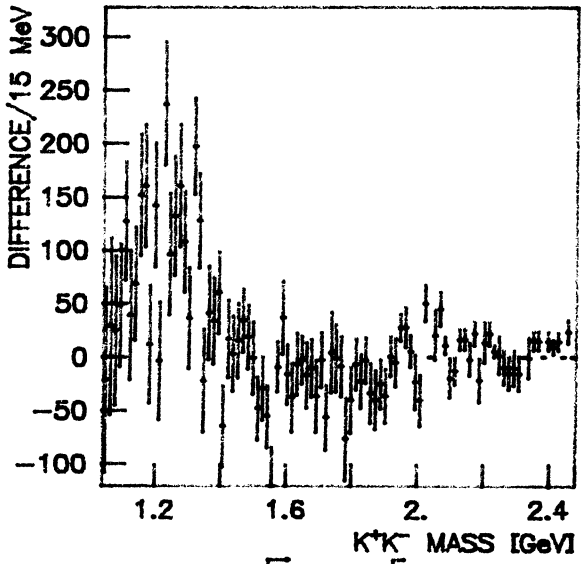

Figure 5

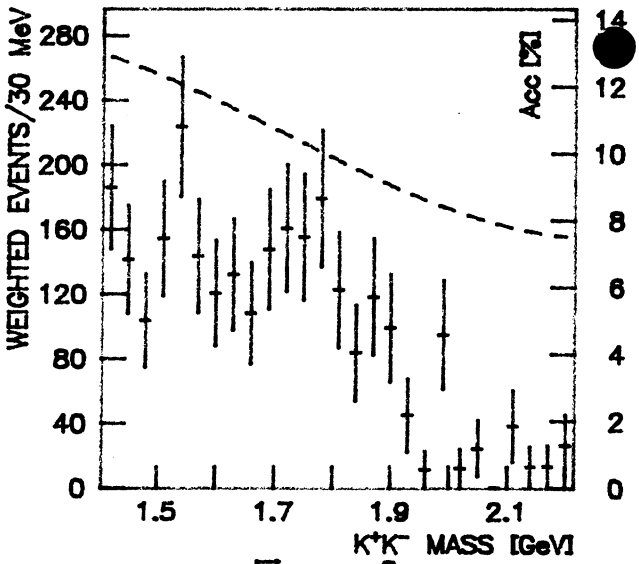

Figure 6a

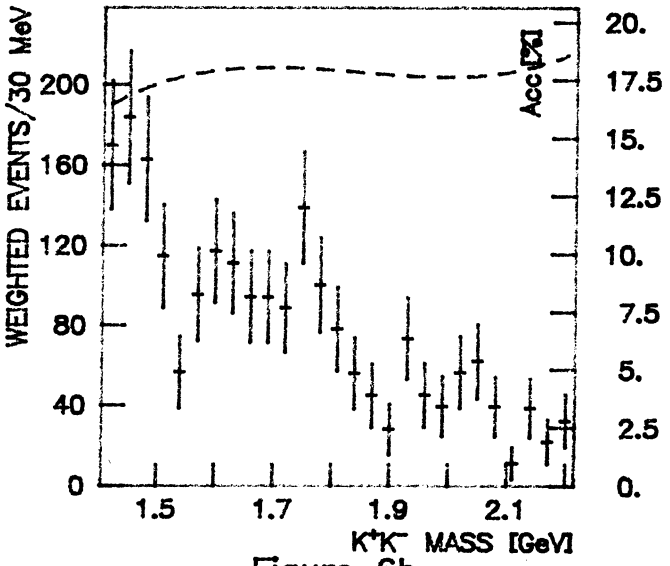

Figure 6b

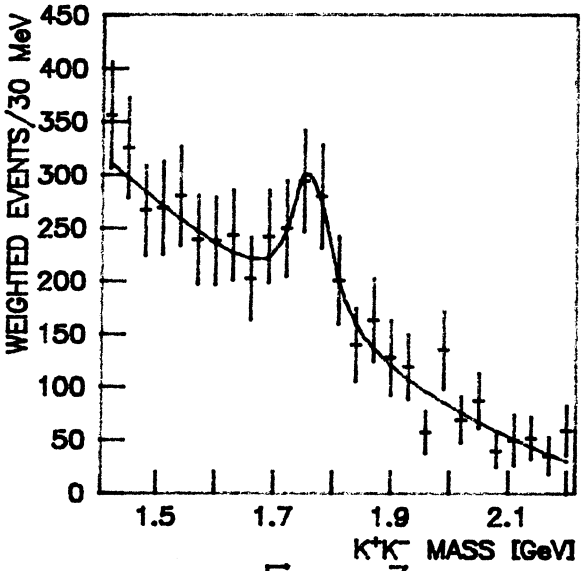

Figure 7